Petrology and mineralogy of the angrite Northwest Africa 1670

Albert Jambon, Omar Boudouma, Michel Fonteilles, C. Le Guillou, D. Badia, Jean-Alix J-A Barrat

The Meteoritical Society

Meteoritics & Planetary Science 43, Nr 11, 1783–1795 (2008)
Abstract available online at http://meteoritics.org

Petrology and mineralogy of the angrite Northwest Africa 1670

A. JAMBON[1*], O. BOUDOUMA[2], M. FONTEILLES[3], C. LE GUILLOU[4], D. BADIA[1], and J.-A. BARRAT[5]

[1]Laboratoire Magie, Université Pierre et Marie Curie-Paris 6 and IPGP, CNRS UMR 7154, case 110, 4 place Jussieu, 75252 Paris cedex 05, France
[2]Service du MEB, UFR des Sciences de la Terre, Université Pierre et Marie Curie-Paris 6, case 110, 4 place Jussieu, 75252 Paris cedex 05, France
[3]Pétrologie, Modélisation des Matériaux et Processus, CNRS UMR 7160 Université Pierre et Marie Curie-Paris 6, case 110, 4 place Jussieu, 75252 Paris cedex 05, France
[4]Laboratoire de Géologie, ENS, CNRS UMR 8538, 24 rue Lhomond, 75005 Paris, France
[5]UBO-IUEM, CNRS UMR 6538, Place Nicolas Copernic, F29280 Plouzané, France
[*]Corresponding author. E-mail: albert.jambon@upmc.fr

(Received 27 March 2007; revision accepted 4 June 2008)

Abstract–Northwest Africa (NWA) 1670, contains olivines of up to 5 mm in size representing about 30% of the studied section. With subordinate clinopyroxene and chrome-spinel microphenocrysts (0.2–0.5 mm), they represent a xenocrystic association. Phenocrysts are surrounded by a groundmass, predominantly comprising bundles of plagioclase and clinopyroxene (typically 20×200 μm crystals). Olivine and kirschsteinite are present in the groundmass in lesser amounts. The olivine xenocrysts (Fo90) are significantly fractured and show mosaicism for their major part, the remaining showing faint undulatory extinction. They are surrounded with a rim of 100–200 μm zoned down to Fo80 and overgrown with serrated olivine, Fo80 to Fo60 (about 100 μm). Olivine in the groundmass is zoned from Mg# 0.55 to 0.15; its CaO content ranges 2.0 to 8.4%. Subcalcic kirschsteinite is zoned from Mg# 0.13 to 0.03, CaO increasing from 15.8 to 21.3%. Pyroxenes xenocrysts (Mg# = 0.77) are superseded in the groundmass by less magnesian pyroxenes, Mg# 0.61 to 0.17, with an average FeO/MnO of 98. Their compositions range from $En_{30}Fs_{22}Wo_{27}Al\text{-}Ts_{28}Ti\text{-}Ts_2$ to $En_2Fs_{37}Wo_{22}Al\text{-}Ts_{40}Ti\text{-}Ts_1$. Anorthite microcrysts (An99-100) are restricted to the groundmass. Accessories are pyrrhotite, kamacite, Ca-phosphate, titanomagnetite, hercynite and Ca-carbonate.

The bulk chemical composition confirms that NWA 1670 corresponds to a normal angrite melt that incorporated olivine. High Mg olivine xenocrysts and the associated mineralogy are typical of angrites. We suggest that it is an impact melt with relict phenocrysts. The strong silica undersaturation, the presence of Fo90 olivine xenocrysts and carbonate support their derivation as melilite-like melts in the presence of carbonate.

INTRODUCTION

Angrites constitute a grouplet of achondrites (one fall and nine finds), the petrogenesis of which remains controversial (e.g., Prinz et al. 1977; Mittlefehldt et al. 1990, 1998, 2002; Prinz and Weisberg 1995; Varela et al. 2003; Kurat et al. 2004; Jambon et al. 2005). Following the early experimental work of Jurewicz et al. (1993), it was proposed that they were partial melts derived from CV chondrites formed at an oxygen fugacity of IW + 2. Varela et al. (2003) and Kurat et al. (2004) from their study on D'Orbigny suggested that they were rather nebular condensates. From a study of Northwest Africa (NWA) 1296 (Jambon et al. 2005), it has been suggested that angrites are typical achondrites that were generated by melting under pressure in the presence of carbonate, such as terrestrial melilitic magmas, a unique case among achondrites. In order to assess the merits of the different models, investigations of new angrite specimens is important.

In this paper, we will limit our study to a petrological and mineralogical description. The geochemical aspects will be restricted to the major elements.

NWA 1670 is a small (29 g) stone found in the north African desert (exact location unknown) and bought by a dealer in Erfoud (Morocco) in the spring of 2001. The fusion crust is nearly absent and altered but the inside does not show evidence of significant terrestrial weathering. It was studied on a single thin section by optical examination, scanning electron microscopy (SEM), and electron microprobe analysis (EMPA) in Paris.

Backscattered electron (BSE) imagery reveals numerous

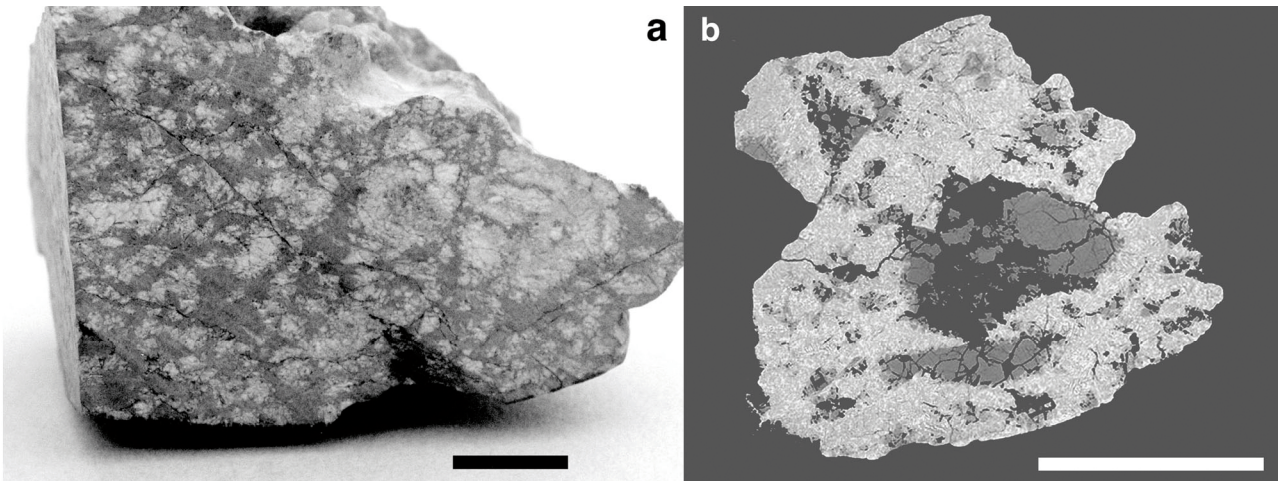

Fig. 1. a) View of the sawn surface showing the abundant olivine xenocrysts surrounded by the dark matrix; scale bar 5 mm. b) Composite BSE image showing the whole section studied in this report; scale bar 5 mm. Notice the large olivine crystals in the center (light gray) partly lost during sample preparation.

light gray olivine crystals several millimeters in size in a light gray fine grained groundmass (Fig. 1). During sample preparation, portions of highly fractured olivines were lost, explaining the significant space in the thin section.

Here we report on the mineralogy and petrology of this new angrite find, make comparisons with the other known angrites, and discuss their likely petrogenesis.

Analytical Methods

The rock was cut with a diamond wire saw using ethanol as a lubricant to recover a 4 g slice from which a thin section was prepared. Spare cutoffs were saved for chemical analysis.

Optical observations and quantitative chemical analysis of the various phases were made on a thin section of NWA 1670 of about 1.05 cm^2. The procedures are similar to those used for the angrite NWA 1296 (Jambon et al. 2002, 2005). BSE images were taken with a JEOL 840A scanning electron microscope with an accelerating voltage of 15 KV, and using an energy dispersive spectrometer (EDS) with a resolution of 129 eV. Electron microprobe analyses were obtained with a Cameca SX100 (WDS). Operating conditions were: 15 kV accelerating voltage with a probe current of 12 nA and a spot size of about 1 μm for all phases. Estimating Fe^{3+} in pyroxenes and plagioclase is a difficult task as the result incorporates all the errors on the other cations.The correlation with Al obtained in plagioclase and the nearly constant value in pyroxene suggest that the error on Fe^{3+} does not exceed 0.1 atom p.f.u in plagioclase and 0.03 in pyroxene. In the case of carbonates, C was not analyzed, but its presence was qualitatively checked with the EDS analyzer, as the C peak due to C coating is several times smaller than that observed in carbonates, and the absence of other components (like SO_3 or P_2O_5) is controlled as well.

The modal composition has been estimated by point counting using BSE images. In addition, the amount of olivine crystals has been estimated on a picture of the sawn surface (Fig. 1a).

Sawn surfaces and outer crust were discarded in preparing a split for chemical analysis. A 500 mg fragment was finely ground using a sapphire mortar and pestle. A split (100 mg) was used to determined the major abundances by inductively coupled plasma–atomic emission spectrometry (ICP-AES). The procedures are similar to those used for other achondrites (Barrat et al. 2002a, 2002b; Jambon et al 2002). According to the chemical procedures (dissolution in HF), SiO_2 can only be obtained by difference after analysis of all the major components. Duplication of previous results using different procedures in several other laboratories indicates that no significant error is introduced this way.

RESULTS AND DISCUSSION

Petrography

Optical Examination

The size of the olivine crystals is quite variable from a few hundred micrometers to five millimeters. In principle, one should make the distinction between xenocrysts and phenocrysts, but as is shown below, this is nearly impossible. Olivine xenocrysts make up the cores of the crystals. They exhibit mosaicism in domains of 50–100 μm and show undulatory extinction in their rims. Their xenocrystic nature can be deduced from the texture and composition (see below). Overgrowths of olivine around the xenocrystic cores are revealed by their different compositions; they appear undeformed. Large olivine crystals in the section represent about 30 vol% after correction for the voids which amount to about 10%. Olivine xenocrysts and pyroxene microphenocrysts are highly fractured, with groundmass

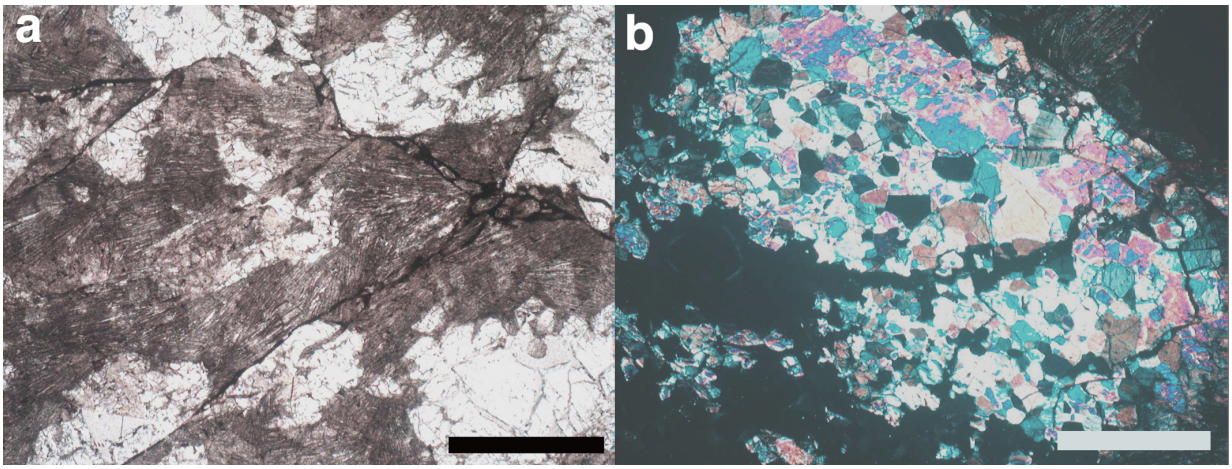

Fig. 2. a) Photomicrograph showing olivine microphenocrysts with their overgrowth surrounded by bundles of micrometric needles of anorthite, clinopyroxene, and olivine not to be distinguished under the optical microscope. b) Olivine phenocryst; crossed polars. Notice the mosaicised and fractured character of the crystal; scale bar 1 mm.

intruding into the largest fractures, some of which have been partly healed to yield melt pockets. Olivines contain micrometric inclusions of sulfide, which possibly mark the pathways of former healed fractures. The olivine rims are always overgrown with a thin margin, and sometimes with tooth-shaped olivine overgrowth protruding into the groundmass. In the groundmass, small skeletal olivine phenocrysts (on the order of 100 μm) appear to be the equivalent of the overgrowths on the xenocrysts, according to their texture and composition.

There are only few pyroxene phenocrysts compared to olivine. They are significantly smaller, with little or no overgrowth. They always occur in close contact with olivine xenocrysts. They appear to be idiomorphic with a losangic shape. Their zoning is less pronounced than that of olivines.

Hercynitic spinel microphenocrysts are also present in this set of xenocrystic phases. They always occur in close contact with olivine xenocrysts. Some of them are broken with fractures filled with groundmass, spinel in the groundmass having a different composition.

The rock is highly fractured and according to the texture, some of the fractures were formed after the onset of groundmass crystallization and before complete solidification.

SEM Examination

Because of the small size of the groundmass crystals, BSE examinations were necessary to achieve a complete and accurate inventory of all mineral phases and their mutual relationship. The groundmass represents the major part of the rock (about 69 vol%).

All phases are intimately mixed with pyroxene, olivine, and plagioclase forming bundles of elongated crystals with a width of less than 10 μm.

Anorthite appears to be the most significant phase, which controls the groundmass texture. Cloudy crystals are widespread, melt inclusions resulting from partly healed skeletic crystals (cf. Lofgren 1974). The association of chains of olivine and anorthite microcrysts typical and systematic in NWA 1296, observed to a lesser extent in Sahara 99555 are met in a few instances in the groundmass. There is no clear evidence as to their relationship to the cloudy laths of anorthite.

Minor accessories such as pyrrhotite, Ca-phosphate, Ti-magnetite are always very small at the limit of analytical determination. Minor kirschsteinite is present as revealed by analytical determination only. According to the texture, titanomagnetite and Ca-silico-phosphates appear late in the crystallization sequence. Small spherules of iron (a few micrometers in diameter) have also been observed revealing the reduced character of this magma up until the end of crystallization, as observed in NWA 1296 (Jambon et al. 2005).

Spinels in the groundmass differ significantly from those described above as xenocrysts. Their composition is similar to that of the spinel microcrysts in D'Orbigny (Mittlefehldt et al. 2002).

Terrestrial carbonate was not observed in the studied section. As primary carbonate was observed in NWA 1296, D'Orbigny and Sahara 99555 (Jotter et al. 2002; Kurat et al. 2004; Jambon et al. 2005), we performed a search specifically for carbonate in NWA 1670. We did observe neither vesicles nor fractures filled with carbonate. Instead in a specific part of the section we observed a number of spherical or ovoid carbonate inclusions in pyroxene (Fig. 3d). Their sizes range from less than one micrometer up to 5 micrometers for the largest one. In addition, a number of empty cavities are interpreted as carbonate lost during sample preparation. Since no carbonate filled fractures are observed, these spheres are interpreted as immiscible carbonate droplets trapped in the pyroxene.

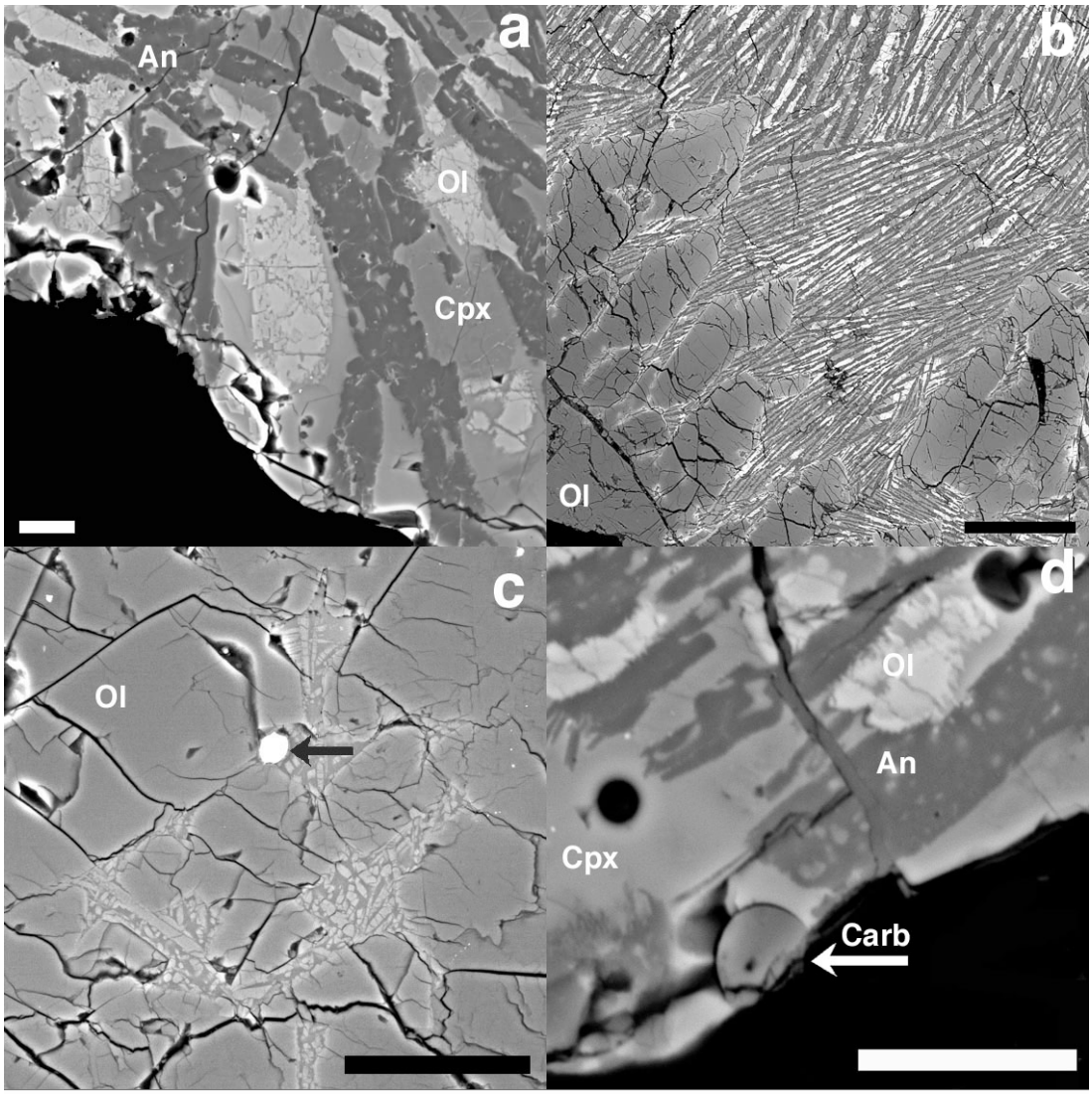

Fig. 3. BSE images showing details of the texture. a) Poorly crystallized anorthite laths (dark gray) surrounded by clinopyroxene and olivine; scale bar 10 μm. b) Olivine overgrowth around the xenocrysts. Notice the sharp zoning at the edges. White laths in the groundmass are fayalite rich olivine and kirschsteinite. Dark laths are anorthite surrounded by gray pyroxene. Notice the fractured character of the overgrowths compared to the groundmass. Scale bar 0.2 mm. c) Interstitial melts within the fractures of olivine phenocrysts. Notice the white sulfide globule (arrow). Scale bar 0.1 mm. d) Close up showing carbonate droplets included in clinopyroxene. One is empty (black) the other at the rim of the sample is incomplete. Scale bar 10 μm.

Mode

The mode was estimated from BSE images at two magnifications. At low magnification (×15) we counted the xenocrysts and the voids. At higher magnification (×50) we could separate the microcrysts in the groundmass. Determining the mode of this rock is quite difficult for a number of reasons. According to their composition and to the texture, most of the olivines are xenocrysts. A significant fraction was lost during sample preparation, but we cannot be certain that olivine alone was lost. This rock is actually a mixture of overgrown xenocrysts (mostly olivine) and fine grained groundmass. According to the grain size of the phenocrysts (nearly one cm for the size of the aggregates) it is not possible to observe a surface area large enough with respect to the overall size of the specimen. From image processing we estimate the amount of olivine xenocrysts in the section at 20 vol% but this estimate cannot be accurate because of the impossibility to separate xenocrysts from their overgrowths (about 1–2%). The voids amount to 10%, which could be counted as additional xenocrysts. In the groundmass pyroxene accounts for 27%, anorthite for 32%, fayalite-rich olivine (and kirschsteinite) for 9%, and opaques for less than 1%.

Because of the difficulties in estimating the mode, we counted the groundmass on the picture of the sawn surface

Table 1. Representative analyses of olivine and kirschsteinite.

	Olivine						Kirschsteinite	
	Core		Overgrowths		Groundmass		Groundmass	
#	*9/11*	*897*	*1323*	*794*	*991*	*8/5*	*66*	*53*
SiO_2	40.95	39.47	38.56	35.63	31.67	31.65	29.85	29.87
TiO_2	0.04	0.09	0.03	0.10	0.11	0.18	0.11	0.19
Al_2O_3	0.06	0.15	0.11	0.20	0.05	0.29	0.07	0.00
Cr_2O_3	0.37	0.22	0.16	0.03	0.02	0.00	0.00	0.00
MgO	48.38	42.11	38.46	26.69	8.39	4.44	3.72	1.04
FeO	9.63	16.98	21.21	33.92	53.03	52.12	46.24	44.46
MnO	0.16	0.14	0.15	0.32	0.77	0.73	0.62	0.37
CaO	0.37	0.54	0.61	1.32	3.92	10.22	15.83	20.65
Na_2O	0.02	0.02	0.00	0.01	0.02	0.00	0.02	0.00
Total	99.96	99.76	99.35	98.29	98.06	99.64	96.74	96.93
Mg#	0.90	0.82	0.76	0.58	0.22	0.13	0.13	0.04

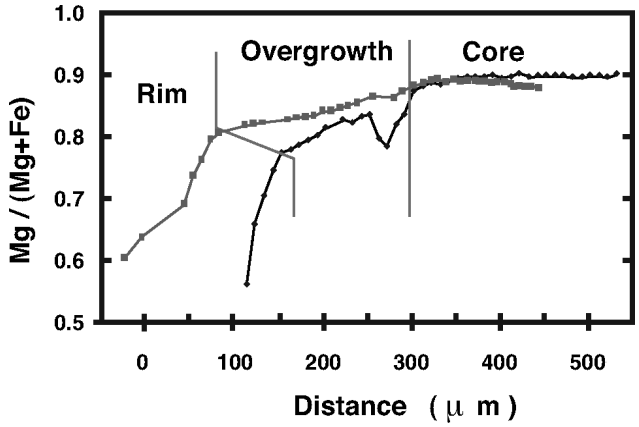

Fig. 4. Two examples of zoning at the rim of an olivine xenocryst. The cores exhibit the same composition for all the large xenocrysts. Notice the fracture between the core and the overgrowth (see Fig. 2a).

(Fig. 1a). We obtain 82% for the groundmass, which is probably a fair estimate of the average value because of the large surface area considered (4 cm^2).

In principle, this mode can be checked from the bulk rock analysis. This again is difficult since olivine and pyroxene exhibit strongly variable compositions.

Mineral Compositions

Major mineral compositions determined by EMPA are reported in Tables 1–4.

Olivines

The diverse olivine types exhibit different compositions (Fig. 4, Table 1). Xenocrysts display homogenous cores at Fo90 with little Ca and Cr. Overgrowths are in the range Fo85-75 and rims decrease to Fo55. The CaO content of olivine increases with its Fa content (Fig. 5) and reaches 1% at Fo55. Olivine zoning extends over a distance of at least 0.2 mm up to one millimeter. Olivines in the groundmass are even more enriched in iron (Fo15), with CaO values of 15%. Small crystals of subcalcic kirschsteinite (10 μm at most) with Ca up to 0.75 atom p.f.u. occur in the groundmass.

Pyroxenes

Pyroxenes, as in the angrites, are Al-rich diopside-hedenbergite solid solutions (fassaite; Table 2). They are zoned from core to rim in the microphenocrysts (Fig. 6). Pyroxene compositions have been calculated for 4 cations and 6 oxygens which permits estimations of Fe^{2+} and Fe^{3+}. Their compositions are calculated taking into account the Ti and Al Tschermak (Ts) components. Projection from the latter into the En-Fs-Wo plane is presented in Fig. 7. Xenocryst core compositions are constant at $Ti\text{-}Ts_1Al\text{-}Ts_{18}En_{33}Fs_9Wo_{40}$. The compositions of the overgrowths and in the groundmass vary significantly from $Ti\text{-}Ts_3Al\text{-}Ts_{22}En_{30}Fs_{14}Wo_{30}$ to $Ti\text{-}Ts_9Al\text{-}Ts_{10}En_9Fs_{36}Wo_{36}$ for the extreme groundmass compositions. These compositions are high in Tschermak components, especially when compared to the other angrites, the only achondrites containing high Al pyroxene, but the crystals are zoned. The FeO/MnO ratio of individual analyses is highly variable even though this ratio ranges between 60–70 on average in the low range of that measured for pyroxenes of angrites (Mikouchi et al. 1995; Mittlefehldt et al. 2002; Jambon et al. 2005). This high variability of single analyses was already observed in NWA 1296.

It is worth noticing that the Mg# of pyroxene cores is only 0.76, apparently out of equilibrium with the olivine xenocryst cores. The overgrowths are in equilibrium with the groundmass where their Mg# never exceeds 0.24 (in contrast to olivine). Cr never exceeds 0.03 atom p.f.u. in the cores and decreases towards the rims. Fe^{3+} in the pyroxene is extremely limited unlike what was observed in NWA 1296. The pyroxene cores, despite a constant Mg#, exhibit some zoning, with the lowest Tschermak component in the very core (Fig. 8).

The maximum value of the Al-Ts may correspond to the onset of anorthite crystallization in agreement with the interstitial position of plagioclase. Ti varies only marginally except in the very late crystals.

Table 2. Representative analyses of clinopyroxenes. Average and standard deviation (σ) for 25 analyses.

	Cores					Overgrowths				Groundmass	
	522	*426*	*349*	*Average*	σ	*12/13*	*14/26*	*14/49*	*13/43*	*1007*	*1402*
SiO_2	47.87	46.78	45.91	47.57	0.63	46.22	43.18	43.21	45.90	45.39	40.43
TiO_2	1.65	1.91	1.78	1.70	0.20	1.19	1.31	1.46	1.56	2.37	3.55
Al_2O_2	7.23	8.43	9.07	7.56	0.67	10.47	15.93	14.12	8.36	6.81	7.75
Cr_2O_2	0.26	0.31	0.33	0.27	0.13	0.81	0.22	0.27	0.22	0.11	0.06
MgO	11.89	11.41	11.00	11.81	0.30	10.60	8.75	8.40	7.73	6.69	3.80
FeO	6.19	6.85	6.82	6.63	0.34	9.20	8.39	10.50	13.34	15.19	20.81
MnO	0.11	0.02	0.08	0.08	0.06	0.20	0.11	0.13	0.14	0.26	0.19
CaO	24.62	24.29	24.69	24.66	0.23	21.04	21.79	21.57	22.09	22.80	21.76
Na_2O	0.04	0.00	0.05	0.02	0.02	0.00	0.02	0.00	0.01	0.05	0.03
Total	99.93	100.03	99.90	100.38	0.60	99.73	99.70	99.67	99.37	99.96	98.90
Mg#	0.77	0.75	0.74	0.76	0.01	0.67	0.65	0.59	0.51	0.44	0.24
FeO/MnO	54	442	81	83	556	46	75	83	93	59	118
Structural formula calculated for 4 cations and 6 oxygens											
Si	1.78	1.75	1.72	1.77	0.02	1.74	1.62	1.63	1.77	1.77	1.64
Al IV	0.22	0.25	0.28	0.23	0.02	0.26	0.38	0.37	0.23	0.23	0.36
Al VI	0.10	0.12	0.12	0.10	0.01	0.20	0.32	0.26	0.15	0.08	0.01
Fe^{3+}	0.01	0.01	0.04	0.02	0.02	0.00	0.00	0.01	0.00	0.02	0.04
Fe^{2+}	0.19	0.20	0.17	0.18	0.02	0.29	0.26	0.32	0.43	0.48	0.65
Mn	0.00	0.00	0.00	0.00	0.00	0.01	0.00	0.00	0.00	0.01	0.01
Cr	0.01	0.01	0.01	0.01	0.00	0.02	0.01	0.01	0.01	0.00	0.00
Ti	0.05	0.05	0.05	0.05	0.01	0.03	0.04	0.04	0.05	0.07	0.14
Mg	0.67	0.64	0.62	0.66	0.02	0.59	0.49	0.47	0.44	0.39	0.20
Ca	0.98	0.97	0.99	0.98	0.01	0.85	0.88	0.88	0.92	0.95	0.96
En	0.33	0.32	0.31	0.33	0.01	0.30	0.24	0.24	0.22	0.19	0.10
Fs	0.09	0.10	0.08	0.09	0.01	0.14	0.13	0.16	0.22	0.24	0.32
Wo	0.41	0.39	0.38	0.40	0.01	0.30	0.25	0.27	0.35	0.38	0.35
Al-Ts	0.16	0.19	0.22	0.18	0.02	0.22	0.33	0.29	0.17	0.12	0.11
Ti-Ts	0.01	0.01	0.01	0.01	0.00	0.03	0.04	0.04	0.05	0.07	0.14

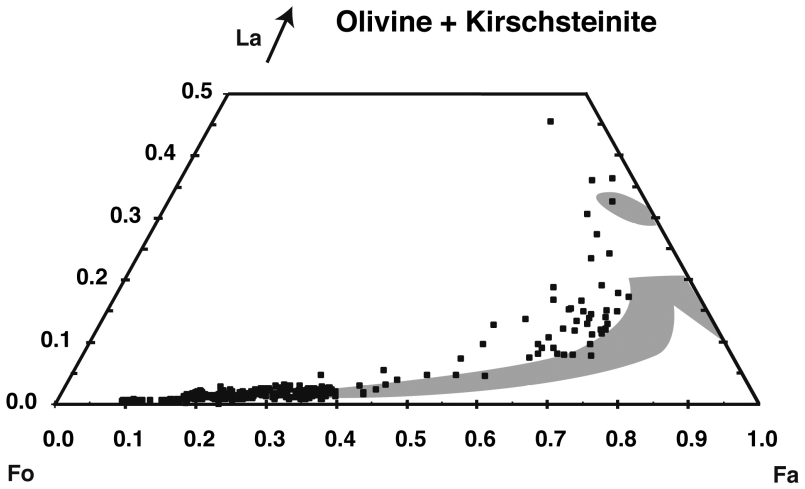

Fig. 5. Olivine compositional plane showing the strongly variable composition of the olivines including the larnite (La) component. Some subcalcic kirschsteinite is also present in the groundmass. The grey field corresponds to olivine compositions in both D'Orbigny and NWA 1296 (Mittlefehldt et al. 2002; Jambon et al. 2005).

Anorthite

Plagioclase is nearly pure anorthite, another feature shared with all angrites. It never occurs as phenocrysts, being found only in the groundmass. Representative analyses are reported in Table 3. This anorthite, however, does display anomalous compositions, some Al deficiency being correlated with excess Fe and Ti (Fig. 9). As noticed by Varela et al. (2003) the Fe/Al substitution could be a feature that characterizes angrites. Contamination from the surrounding groundmass during analysis or because of submicrometric

Table 3. Representative compositions of plagioclase. Average and standard deviation (σ) for 160 analyses.

	599	*498*	*934*	*683*	*996*	*Average*	σ
SiO_2	43.44	43.38	43.16	43.24	41.12	43.04	0.89
TiO_2	0.00	0.07	0.25	0.72	1.32	0.25	0.20
Al_2O_3	36.27	34.83	31.59	29.18	22.79	31.89	1.95
Cr_2O_3	0.07	0.00	0.00	0.05	0.04	0.03	0.03
MgO	0.53	0.19	0.90	0.96	0.27	0.60	0.35
FeO	0.06	1.11	4.06	6.13	12.61	3.39	1.68
MnO	0.00	0.03	0.00	0.05	0.04	0.04	0.04
CaO	20.46	19.68	19.63	19.88	19.69	19.65	0.38
Na_2O	0.10	0.03	0.00	0.01	0.00	0.02	0.02
K_2O	0.01	0.01	0.00	0.00	0.02	0.01	0.01
P_2O_5	0.00	0.19	0.34	0.22	0.40	0.28	0.07
Total	100.99	99.52	99.93	100.43	98.31	99.19	1.20
Mg#	0.17	0.23	0.28	0.22	0.04	0.24	0.09
Structural formula based on 5 cations and 8 oxygens							
Si	2.00	2.03	2.03	2.04	2.03	2.03	0.03
Al	1.97	1.92	1.75	1.62	1.33	1.77	0.10
Fe^{3+}	0.02	–0.02	0.12	0.23	0.47	0.12	0.08
Fe^{2+}	0.01	0.06	0.04	0.01	0.05	0.01	0.03
Mg	0.00	0.01	0.06	0.07	0.02	0.04	0.02
Ca	1.01	0.99	0.99	1.01	1.04	1.00	0.02
P	0.00	0.01	0.01	0.01	0.02	0.01	0.00
tet	3.99	3.94	3.91	3.90	3.85	3.94	0.03
An	0.990	0.998	0.997	0.998	1.000	0.998	0.002
Ab	0.009	0.002	0.003	0.002	0.000	0.002	0.002
Or	0.001	0.000	0.000	0.000	0.000	0.000	0.001

Table 4. Average phosphate analysis (n = 4).

	Average
SiO_2	6.77
TiO_2	0.36
Al_2O_3	0.83
MgO	0.38
FeO	10.16
CaO	42.92
P_2O_5	34.39
SO_2	0.34
F	0.09
Cl	0.07
Total	96.58

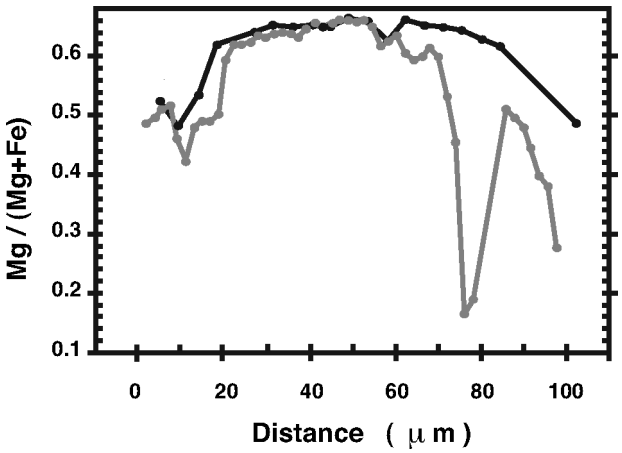

Fig. 6. Rim zoning of two pyroxenes. Notice the sharp profile compared to olivine. The pyroxene cores appear out of equilibrium with the olivine cores. Fracturing (at 75 μm) clearly postdates zoning.

inclusions in the cloudy crystals of anorthite (see Fig. 3) has been considered but seems unlikely to explain these odd compositions (up to 12% FeO). The structural formula is very close to the theoretical one with 1.00 atom Ca p.f.u. Iron appears to be Fe^{3+} in tetrahedral coordination. The abundance of Ti is limited but appears to correlate with Fe while Mg does not. These compositions are the most iron-rich reported so far from angrites. This can be compared with the composition of anorthite in NWA 1296, where FeO is concentrated at the onset of crystallization and disappears afterwards (Jambon et al. 2005). The major difference is that crystallization of anorthite in NWA 1296 stopped before complete crystallization of the rock. It happens that Fe^{3+} in NWA 1296 is incorporated in clinopyroxene especially at the end of crystallization. Here, during the final stage of crystallization, clinopyroxene and anorthite in the groundmass crystallize simultaneously. The deficiency in aluminum is revealed in anorthite rather than in clinopyroxene.

Phosphates

Phosphates are very small (typically 1 × 5 μm or less), which precludes high quality analyses. An average

Table 5. Representative compositions of spinels.

	Xenocrysts		Overgrowths		Groundmass		
	1/1	*29*	*67*	*6/1*	*18/1*	*2/1*	*61*
SiO_2	0.19	0.32	0.15	0.32	2.38	0.27	0.34
TiO_2	0.28	1.14	3.47	4.29	11.33	18.23	29.33
Al_2O_3	53.31	49.68	43.43	41.23	18.08	14.61	1.99
Cr_2O_3	10.88	10.82	9.09	7.36	15.23	6.94	0.00
MgO	14.47	11.27	5.97	3.64	3.02	1.92	0.18
FeO	19.27	24.29	35.92	40.48	43.54	53.14	64.11
MnO	0.22	0.16	0.35	0.20	0.31	0.36	0.21
CaO	0.05	0.09	0.17	0.19	0.79	0.33	0.52
Total	98.68	97.84	98.57	97.79	94.77	95.86	96.70
Mg#	0.57	0.45	0.23	0.14	0.11	0.06	0.00
Structural formula based on 3 cations and 4 oxygens							
Mg	0.59	0.48	0.27	0.17	0.16	0.10	0.01
Mn	0.01	0.01	0.01	0.01	0.01	0.01	0.01
Ti	0.01	0.02	0.08	0.10	0.31	0.49	0.84
Fe^{2+}	0.41	0.54	0.81	0.12	0.17	0.21	1.83
Fe^{3+}	0.03	0.04	0.09	0.93	1.15	1.39	0.22
Cr	0.24	0.24	0.22	0.18	0.44	0.20	0.00
Al	1.72	1.67	1.54	1.50	0.77	0.62	0.09
Ulvöspinel	0.01	0.02	0.08	0.1	0.31	0.49	0.84
Magnetite	0.01	0.02	0.05	0.06	0.09	0.10	0.11
Chromite	0.12	0.12	0.11	0.09	0.22	0.10	0.00
Spinel	0.59	0.48	0.27	0.17	0.16	0.10	0.01
Hercynite	0.27	0.36	0.50	0.58	0.22	0.21	0.03

composition is reported in Table 4. The presence of silicophosphate has been mentioned in four other angrites: Asuka (A-) 881371 (Prinz and Weisberg 1995; Warren and Davis 1995), D'Orbigny and Sahara 99555 (Mikouchi et al. 2001; Mittlefehldt et al. 2002; Kurat et al. 2004), NWA 1296 (Jambon et al. 2005). Abundant silica in phosphate is a characteristics of angrites. Notice the very low amounts of Cl and F and the high FeO content.

Oxides

The oxides exhibit strongly variable compositions (Table 5). The first kind is probably xenocrystic as it is rich in spinel component (up to 59 mol%) and associated with olivine xenocrysts. Notice that the same kind of aluminous spinel has been described previously in D'Orbigny (Mittlefehldt et al. 2002) and recognized as xenocrystic. It becomes enriched in hercynitic component (>50 mol%) as crystallization proceeds with minor overgrowths rimming the xenocrysts. Finally, microcrysts of ulvöspinel are found in the groundmass. The chromite-rich rims described in D'Orbigny (Mittlefehldt et al. 2002) are not observed in NWA 1670.

Minor Phases

Small troilite crystals are pure FeS. Metal is the product of exsolution from a sulfide melt. As in NWA 1296 it is partly oxidized, probably following terrestrial alteration. It contains variable amounts of Ni (2–6%); this can be compared with the analyses in D'Orbigny reported by Kurat et al. (2004).

Table 6. Representative carbonate analyses.

	38/9	*38/5*	*38/8*	*Average*	*Sigma*
SiO_2	0.23	0.08	0.01	0.12	0.08
FeO	0.89	0.51	0.35	0.49	0.22
CaO	54.71	55.47	55.10	55.03	0.37
Na_2O	0.07	0.04	0.00	0.05	0.05
K_2O	0.00	0.03	0.04	0.03	0.02
CO_2[a]	43.54	43.90	43.51	43.53	0.32
Total	99.45	100.03	99.03	99.25	0.74

[a]CO_2 calculated by stoichiometry. Average and standard deviation for 7 analyses.

calculated by stoichiometry because of the limited precision on both O and C, which can be qualitatively detected with the EDS analyzer of the microprobe. It is important to notice that neither MgO nor FeO are significant components in the carbonate unlike what is observed in the martian pyroxenite ALH 84001, suggesting that the conditions of formation were significantly different.

Major Element Geochemistry

The major element analysis is reported in Table 7. Compositional characteristics of angrites are observed: low SiO_2, high FeO, high FeO/MnO and high CaO/Al_2O_3. The high MgO value compared to NWA 1296, Sahara 99555, D'Orbigny, Lewis Cliff (LEW) 86010 (range of 6.5–7%) results from the abundance of Mg rich olivine

Table 7. Major element composition of angrites. For NWA 1670 and NWA 1296, SiO_2 by difference (see text) and total without SiO_2.

	Picritic angrites			Angrite melts			Cumulate	
	NWA 1670	LEW 87051	Asuka-881371	NWA 1296	LEW 86010	D'Orbigny	SAH 99555	Angra dos Reis
References	1	2	2	3	2	4	4	2
SiO_2	*42.18*	40.40	37.30	*39.54*	39.60	38.40	38.60	43.70
TiO_2	0.67	0.73	0.88	0.93	1.15	0.89	0.91	2.05
Al_2O_3	11.70	9.19	10.10	12.18	14.10	12.40	12.50	9.35
Cr_2O_3	0.14	0.02	0.01	0.07	0.01	0.05	0.05	0.02
MgO	14.60	19.40	14.80	6.71	7.00	6.49	7.04	10.80
FeO	18.52	19.00	24.00	25.00	18.50	24.70	23.10	9.40
MnO	0.22	0.24	0.20	0.28	0.20	0.28	0.26	0.10
CaO	11.95	10.80	12.50	14.65	17.50	15.00	15.10	22.90
Na_2O	0.01	0.02	0.02	0.03	0.02	0.02	0.02	0.03
K_2O	0.03	–	–	<0.03	–	0.01	0.01	–
P_2O_5	0.12	0.08	0.17	0.17	0.13	0.16	0.15	0.13
Total	*57.82*	100.02	100.11	*59.96*	98.32	98.38	97.72	98.68
Mg#	0.58	0.65	0.52	0.32	0.40	0.32	0.35	0.67
FeO/MnO	84	79	120	88	93	88	89	94

[1]This work.
[2]Mittlefehldt and Lindstrom (1990).
[3]Jambon et al. (2005).
[4]Mittlefehldt et al. (2002).

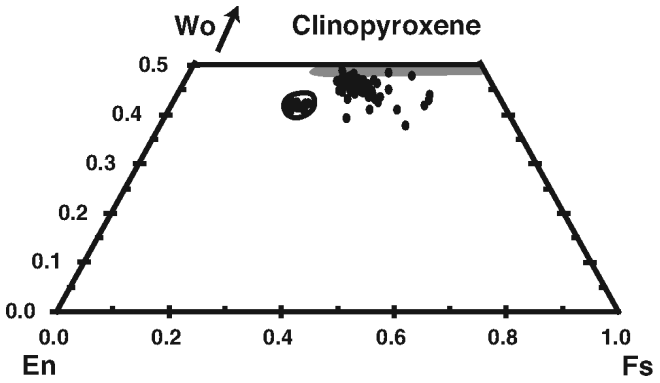

Fig. 7. Pyroxene compositional quadrilateral. Compared to olivine the compositional range is restricted. Notice the high Wo content. Projection from the Tschermak component. The grey field corresponds to pyroxene compositions for D'Orbigny and NWA 1296 (Mittlefehldt et al. 2002; Jambon et al. 2005).

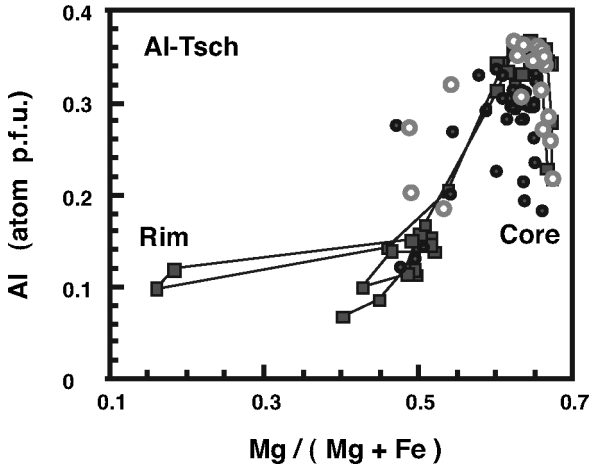

Fig. 8. Distribution of the Al-Tschermak component in clinopyroxene as a function of the Mg#. The initial increase in the core may precede the crystallization of anorthite. Different symbols refer to different crystals; the tie line connects data points for one crystal.

xenocrysts. Actually, A-881371 and LEW 87051, which contain xenocrysts of magnesian olivine, exhibit MgO concentrations of 14.8 and 19.4%, respectively. This can be illustrated in a FeO versus MgO diagram (Fig. 10). All true angritic melts plot at a low MgO value. Picritic angrites, i.e., those containing olivine xenocrysts, can be understood as a mixture of an angritic melt and olivine. In the case of NWA 1670, when substracting 18.2% of olivine of the observed xenocrystic composition (Table 1), we obtain a melt intermediate between NWA 1296-D'Orbigny-Sahara 99555 on the one hand, and LEW 86010 on the other hand. Notice that 18.2% olivine is very close to the modal estimate above, taking proper care of the sampling representativeness. According to Fig. 10, it becomes clear that LEW 87051 and A-881371 relate similarly to the angritic melts, as already advocated previously (Mikouchi et al. 2003) by the addition of xenocrystic highly magnesian olivine. These melt compositions define a trend towards the most magnesian pyroxene analyzed in NWA 1670, but according to Fig. 10, other moderately evolved pyroxenes can also be considered. In addition, Angra dos Reis, a pyroxene cumulate of the angrite clan, plots on the same trend. From this evidence, it is suggested that the different angrites relate to one another by pyroxene accumulation (in

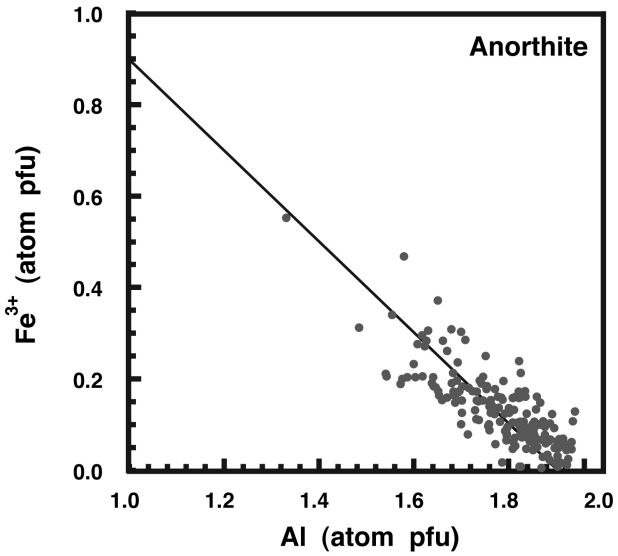

Fig. 9. The correlation of Fe^{3+} with Al in anorthite strongly supports substitution in the tetrahedral site.

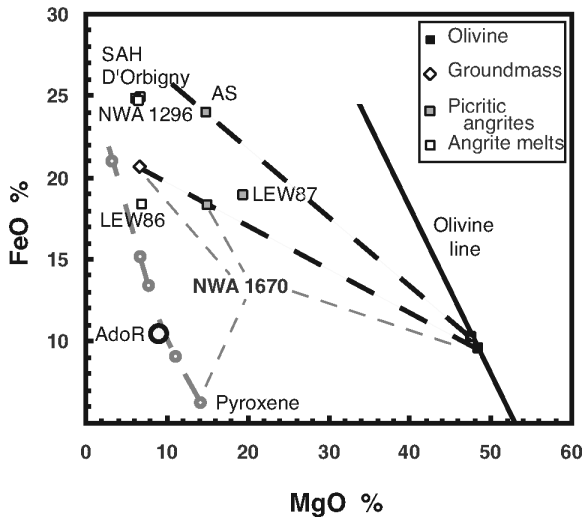

Fig. 10. FeO:MgO diagram. Mass balance permits to derive possible groundmass composition once the bulk rock and olivine compositions are known. Notice that angrites with olivine xenocrysts (picritic angrites) are significantly enriched in MgO relative to pure angritic melts like D'Orbigny. AdoR (Angra dos Reis) a pyroxene cumulate and the pyroxene compositions of NWA 1670, suggest that different angrites relate to one another through pyroxene accumulation.

addition to olivine incorporation). Notice, however, that in the case of very small samples (e.g., A-881371) some analytical bias could result from an unrepresentative sample. The importance of xenocrystic olivine incorporation is confirmed in the plot of Al_2O_3 against CaO (Fig. 11) where a mixing trend between olivine (near the origin) and angritic melts is obvious.

DISCUSSION

NWA 1670 possesses a number of petrological and mineralogical characteristics akin to angrites. These are i) the association of the three major phases: dominant olivine, Al-rich pyroxene and pure anorthite. ii) The olivines include an increasing amount of Ca with decreasing Fo content. iii) In the final stages of crystallization kirschsteinite replaces olivine. iv) Plagioclase is pure anorthite, the rock being devoid of alkalies, both Na and K. The presence of Fe in anorthite was reported in NWA 1296 (Jambon et al. 2005) but not as high as in NWA 1670. v) The pyroxenes exhibit an unusual composition with high Al and Ca contents, expressed in a significant Tschermak component. All these features reflect a high Ca (superchondritic Ca/Al), low SiO_2 content of the bulk rock.

The Al-rich spinel is present in some but not all of the angrites; in D'Orbigny it was interpreted as xenocrystic (Mittlefehldt et al. 2002) and it is likely to be the case in NWA 1670 as well. Highly magnesian xenocrystic olivines have been recognized in other angrites (D'Orbigny, LEW 87051, Asuka-881371), but not in all of them (see also Mittlefehldt et al. 1998). The Mg# of the olivines in NWA 1670 are the most magnesian ever encountered in any achondrite; one similar composition is reported by Kurat et al. (2004) for a megacryst in D'Orbigny. For comparison terrestrial mantle olivines have a Mg# of 0.88 instead of 0.90 in NWA 1670 (notice that the value of 0.92 reported by Mikouchi et al. (2003) is not confirmed). The mosaicised texture and the deformation revealed by undulatory extinction of these olivines suggest that they could be remnants after impact melting.

The occurrence of carbonate in NWA 1670 as in several other angrites is a unique feature among achondrites. We claim that it is a key to understanding their petrogenesis. Another key is the very low silica content of angrites: terrestrial peridotites and mantle olivines contain more silica than bulk rock angrites! A peridotite is an assemblage of dominant olivine, orthopyroxene, clinopyroxene, and a minor aluminous phase (plagioclase, spinel, or garnet). Upon melting at low to moderate pressure, the liquid is basaltic and enriched in silica relative to the source peridotite. Therefore, angrite genesis cannot be explained in this way. An additional oxide phase, low in silica, must be a crucial component during melting. It has been suggested that this could be spinel (Jurewicz et al. 1993; Longhi 1999), which is indeed found in NWA 1670 and in some angrites. Another possibility already suggested by Jambon et al. (2005) is melting in the presence of carbonate.

The Case of Residual Spinel

Jurewicz et al. (1993) investigated this possibility experimentally. The starting composition must be low in silica and high in oxidized iron. Carbonaceous chondrites

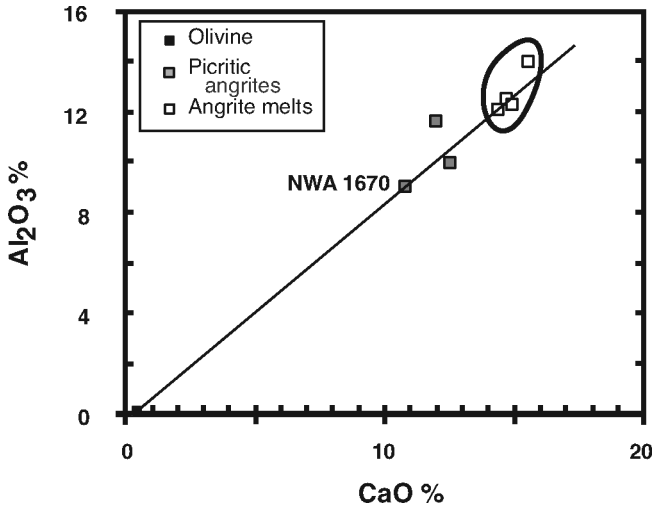

Fig. 11. Al_2O_3:CaO diagram. Picritic angrites plot between olivine at the origin and the angritic melt field, in agreement with a binary mixing corresponding to the incorporation of highly magnesian olivine xenocrysts.

(most likely CV) could provide such compositions. Then an angrite-like melt can be generated under oxidizing conditions (IW + 2) (see also Longhi 1999). Despite its success, the model meets a number of difficulties: 1) highly magnesian olivines cannot be generated under such conditions even if special fractionation conditions are proposed. 2) The oxidizing conditions do not permit the separation of a core. Angrites are depleted in siderophiles (Mittlefehldt et al. 1998, 2002; Kurat et al. 2004) meaning that their parent body had separated a significant core. 3) The CaO content and the Ca/Al ratio do not match that of angrites so well. 4) Angrites are not oxidized melts since, according to its association with sulfide, metal probably results from the exsolution from a sulfide melt, like in NWA 1296 (Jambon et al. 2005) or similarly for nickel-iron (D'Orbigny) (Kurat et al. 2004). 5) Ibitira is a eucrite-like angrite: its mineralogy is eucritic and therefore should be derived from a similar parent under reducing conditions (Jurewicz et al. 1993); according to its oxygen isotopes however, it comes from the same parent body as the angrites, and this parent body must have been thoroughly mixed (Greenwood et al. 2005).

Even if these difficulties may not be sufficient to discard this model definitely, looking at the other possibility seems justified at least.

Melting in the Presence of Carbonate

This possibility, suggested first by Jambon et al. (2005), is obviously supported by the presence of magmatic carbonate which remains unexplained in the previous model and which is specific to angrites. Disproportion of Ca-carbonate to CaO and CO_2 yields the excess calcium required. Terrestrial magmas melted in the presence of carbonate are hyperalcaline magmas commonly associated with carbonatites, e.g., in the East African Rift (see e.g., Demant et al. 1994). These are the silicate magmas with the lowest silica contents (typically 35–40%). If such magmas exist on the Earth why should they not exist on other bodies as well? Such magmas are quite rare on Earth but angrites are rare achondrites too. Melting in the presence of carbonate does not constrain the oxygen fugacity. In this case, a core can be generated as well as highly magnesian olivines. This idea is trivial as it is exactly what happens on the Earth. Basaltic melts (Ibitira composition) can be generated on the same parent body if melting occurs in a more classical way, i.e., from a peridotitic composition sensu lato, with no need to change the oxygen fugacity.

Carbonate, as it disproportionates, buffers the Ca activity at a high level controlling the odd mineralogy observed (fassaitic pyroxene, CaO in olivine and kirschsteinite). Ca is so overabundant that Al is deficient in anorthite (NWA 1670) or pyroxene (NWA 1296) despite the introduction of Ca in olivine.

The puzzling difference with terrestrial melilitic rocks is the absence of alkalies. This might result from the absence of alkalies on the parent body, even more than in the eucrite parent body or the Moon. Another possibility would be alkali loss after impact. As is the case for many achondrites, angrites are possible impact melts (see Mikouchi et al. 2003; Jambon et al. 2005) in agreement with the presence of shocked olivine xenocrysts. Mafic melts loose their alkalies quite easily upon impact (Osinski and Spray 2001) and therefore this is one possible explanation.

The major compositional variations among angrites correspond to the incorporation of highly magnesian olivines. This appears to be a prominent feature if we assume that our present collection of angrites is representative of the group. This incorporation of olivine in itself is not a unique feature; terrestrial oceanic island basalts and shergottites similarly can be basaltic or picritic (e.g., Barrat et al. 2002). A more interesting but as yet unanswered question is whether this feature requires a major parent body as is the case for Mars and Earth. More constraining is the composition of the olivine xenocrysts. They could be residual after partial melting of the mantle or be the first crystallization products after complete melting of the parent body (or any composition in between). These two extreme possibilities constrain the Mg# of the parent body (starting material before melting) to remain in the range 0.90–0.73 if we assume that melts are in equilibrium with the olivine crystals. The Mg# of olivine in the mantle of a planetary body is an indication of the oxidation of iron. Lherzolitic shergottites exhibit a maximum Mg# of 0.76 (McSween and Treiman 1998), whereas terrestrial peridotites exhibit a Mg# of 0.88. The massive metallic core of the Earth is another evidence of its strongly reduced state while the smaller core of Mars indicates a less reduced state. If we follow this line, the parent body of angrites should also be strongly reduced, at least as much as the Earth. It is important

to notice at this point that what is meant here is the average reduction state of the whole body and not the result of late evolution: for instance the eucrite parent body is not as reduced as the Earth if we consider the Mg# of olivines in diogenites, which rarely exceed 0.75. On the other hand, metallic iron is a frequent accessory phase, indicating more reducing conditions than during the genesis of terrestrial basalts.

CONCLUSIONS

NWA 1670 exhibits typical angrite characteristics, including its oxygen isotopes (Greenwood et al. 2005). Its mineralogy is characterized by a Ca overabundance and a very low silica content, unlike melts produced from partial melting of a normal peridotitic composition. The presence of magmatic carbonate supports their petrogenesis by melting in the presence of carbonate, as suggested previously (Jambon et al. 2005). The angrite parent body is, as far as we know, the only body capable of producing such unusual mineralogy and therefore of generating carbonated melts. Since angrites are among the oldest objects in the solar system (Baker et al. 2005; Spivak-Birndorf et al. 2005; Sugiura et al. 2005; Markowski et al. 2006), they might represent the remains of an early stage of planetoid evolution: having expelled their carbonates, planetoids would produce normal basaltic melts as observed on many planets and asteroids.

Editorial Handling—Dr. Randy Korotev

REFERENCES

Baker J., Bizzaro M., Wittig N., Connelly J., and Haack H. 2005. Early planetesimal melting from an age of 4.5662 Gyr for differentiated meteorites. *Nature* 436:1127–1131.

Barrat J.-A., Gillet Ph., Sautter V., Jambon A., Javoy M., Göpel C., Lesourd M., and Petit E. 2002. Petrology and geochemistry of the basaltic shergottite NWA 480. *Meteoritics & Planetary Science* 37:487–500.

Barrat J.-A., Jambon A., Bohn M., Gillet Ph., Sautter V., Göpel C., Lesourd M., and Keller F. 2002. Petrology and geochemistry of the picritic shergottite Northwest Africa 1068 (NWA 1068). *Geochimica et Cosmochimica Acta* 66:3505–3518.

Demant A., Lestrade P., Lubala R. T., Kampunzu A. B., and Durieux J. 1994. Volcanological and petrological evolution of Nyiragongo volcano, Virunga volcanic field, Zaire. *Bulletin of Volcanology* 56:47–61.

Greenwood R., Franchi I., Jambon A., and Buchanan C. 2005. Widespread magma oceans on asteroidal bodies in the early solar system. *Nature* 4351:916–918.

Jambon A., Barrat J. A., Sautter V., Gillet Ph., Göpel C., Javoy M., Joron J. L., and Lesourd M. 2002. The basaltic shergottite Northwest Africa 856: Petrology and geochemistry. *Meteoritics & Planetary Science* 37:1147–1164.

Jambon A., Barrat J.-A., O. Boudouma O., Fonteilles M., Badia D., Göpel C., and Bohn M. 2005. Mineralogy and petrology of the angrite Northwest Africa 1296. *Meteoritics & Planetary Science* 40:361–375.

Jotter R., Jagoutz E., Varela M. E., Zartman R., and Kurat G. 2002. Pb isotopes in glass and carbonate of the D'Orbigny angrite (abstract). *Meteoritics & Planetary Science* 37:A73.

Jurewicz A. J. G., Mittlefehldt D. W., and Jones J. H. 1993. Experimental partial melting of the allende CV and Murchison (CM) chondrites and the origin of asteroidal basalts. *Geochimica et Cosmochimica Acta* 57:2123–2139.

Kurat G., Varela M. E., Brandstätter F., Weckwerth G., Clayton R. N., Weber H. W., Schultz L., Wäsch E., and Nazarov M. A. 2004. D'Orbigny: A non-igneous angritic achondrite? *Geochimica et Cosmochimica Acta* 68:1901–1921.

Lofgren G. E. 1974. An experimental study of plagioclase crystal morphology: Isothermal crystallization. *American Journal of Science* 274:243–273.

Longhi J. 1999. Phase equilibrium constraints on angrite petrogenesis. *Geochimica et Cosmochimica Acta* 63:573–585.

Markowski A., Quitté G., Kleine T., Bizzarro M., Leya I., Wieler R., Ammon K., and Halliday A. N. 2006. Early and rapid differentiation of planetesimals inferred from isotope data in iron meteorites and angrites (abstract). 37th Lunar and Planetary Science Conference. CD-ROM.

McKay G., Lindstrom D., Le L., and Yang S.-R. 1988. Experimental studies on synthetic LEW 86010 analogs. Petrogenesis of a unique achondrite (abstract). 19th Lunar and Planetary Science Conference. pp. 760–761.

McKay G., Crozaz G., Mikouchi T., and Miyamoto M. 1995. Exotic olivine in Antarctic angrites Lewis Cliff 87051 and Asuka-881371 (abstract). *Meteoritics* 30:543–544.

McSween H. Y. Jr. and Treiman A. H. 1998. Martian meteorites. In *Planetary materials*, edited by Papike J. J. Reviews in Mineralogy and Geochemistry, vol. 36. Washington, D.C.: Mineralogical Society of America. pp. 6-1–6-53.

Mikouchi T., Miyamoto M., and McKay G. A. 1996. Mineralogical study of angrite Asuka-881371: Its possible relation to angrite LEW 87051. *Proceedings of the NIPR Symposium on Antarctic Meteorites* 9:174–188.

Mikouchi T., Takeda H., Miyamoto M. Ohsumi K., and McKay G. A. 1995. Exsolution lamellae of kirschsteinite in magnesium-iron olivine from an angrite meteorite. *American Mineralogist* 80: 585–592.

Mikouchi T., Kaneda K., Miyamoto M., Sugiyama K., and Ohsumi K. 2001. Micro Raman spectroscopy of unknown calcium silico-phosphates in angrite meteorites. Eleventh Annual V. M. Goldschmidt Conference.

Mikouchi T., McKay G., Koizumi E., Monkawa A., and Miyamoto M. 2003. Northwest Africa 1670: A new quenched angrite (abstract). *Meteoritics & Planetary Science* 38:A115.

Mittlefehldt D. W. and Lindstrom M. M. 1990. Geochemistry and genesis of the angrites. *Geochimica et Cosmochimica Acta* 55: 77–87.

Mittlefehldt D. W., McCoy T. J., Goodrich C. A., and Kracher A. 1998. Non-chondritic meteorites from asteroidal bodies. In *Planetary materials*, edited by Papike J. J. Reviews in Mineralogy and Geochemistry, vol. 36. Washington, D.C.: Mineralogical Society of America. pp. 4-1–4-195.

Mittlefehldt D. W., Killgore M., and Lee T. 2002. Petrology and geochemistry of D'Orbigny, geochemistry of Sahara 99555 and the origin of angrites. *Meteoritics & Planetary Science* 37:345–369.

Osinski G. R. and Spray J. G. 2001. Impact-generated carbonate melts: Evidence from the Haughton structure, Canada. *Earth and Planetary Science Letters* 194:17–29.

Prinz M., Keil K., Hlava P. F., Berkley J. L., Gómes C. B., and Curvello W. S. 1977. Studies of Brazilian meteorites, III. Origin and history of the Angra dos Reis achondrite. *Earth and Planetary Science Letters* 35:317–330.

Prinz M. and Weisberg M. K. 1995. Asuka-881371 and the angrites: Origin in a heterogeneous, CAI-enriched, differentiated, volatile-depleted body. 20th Symposium on Antarctic Meteorites. pp. 207–210.

Spivak-Birndorf L. Wadhwa M., Janney P. E., and Foley C. N. 2005. Al-Mg isotopic systematics in the angrite Sahara 99555 and the primitive achondrite Brachina (abstract #2201). 36th Lunar and Planetary Science Conference. CD-ROM.

Sugiura N., Miyazaki A., and Yanai K. 2005. Widespread magmatic activities on the angrite parent body at 4562 Ma ago. *Earth, Planets and Space* 57:e13–e16.

Varela M. E., Kurat G., Zinner E., Métrich N., Brandstätter F. Ntaflos T., and Sylvester P. 2003. Glasses in the D'Orbigny angrite. *Geochimica et Cosmochimica Acta* 67:5027–5046.

Yanai K. 1994. Angrite Asuka-881371: Preliminary examination of a unique meteorite in the Japanese collection of Antarctic meteorites. *Proceedings of the NIPR Symposium on Antarctic Meteorites* 7:30–41.